707

SHORT COMMUNICATIONS

J. Appl. Cryst. (1998). **31**, 258–261

On the divergence of rays Bragg diffracted by perfect stationary crystals illuminated with collimated polychromatic radiation

A. R. Lang *at H. H. Wills Physics Laboratory, University of Bristol, Tyndall Avenue, Bristol BS8 1TL, England. E-mail: pharl@siva.bris.ac.uk*

(Received 16 January 1997; accepted 3 September 1997)

Abstract

The properties of three diffraction geometries, *viz* symmetric Bragg-case reflection from a crystal surface, symmetric Laue-case transmission through a parallel-sided crystal and asymmetric Bragg-case reflection from a crystal surface, have been examined under the conditions that the crystal (which is assumed to be perfect) is held in fixed orientation relative to an ideally collimated incident beam of white X-rays. Symmetric Bragg-case reflection has the valuable property of invariant direction of reflected rays for all orders of reflection excited, and for strong and weak reflections alike. For the symmetric Laue case, and for the asymmetric Bragg case approximately, for small asymmetry, expressions are given for the angular range of diffracted rays, scaled in terms of the extinction distance of the reflection concerned. The findings have practical applications in the design and interpretation of continuous-radiation topographic experiments.

1. Introduction

The theory of diffraction by perfect crystals, comprehensively developed though it is, does from time to time require interrogation afresh to provide guidance to experimenters working within the framework of previously unrealized experimental parameters. Such circumstances arise in continuous-radiation synchrotron X-ray topography. This technique is practised most effectively where the combination of small X-ray source dimensions with long distance from tangent point to workstation provides a highly collimated incident beam, with the angular range of rays incident at a point on the specimen crystal being of submicroradian order along one, if not along both, axes normal to the beam. Questions then pertinent are what determines the angular range of the diffracted beam produced by a perfect crystal under such conditions and hence what diffraction/geometrical conditions will provide the sharpest topograph images of a perfect-crystal specimen? Here these questions are investigated for three diffraction geometries: symmetric Bragg-case reflection from a crystal surface, symmetric Laue-case transmission through a parallel-sided crystal plate and asymmetric Bragg-case reflection from a crystal surface.

2. Symmetric Bragg case

Fig. 1 deals with symmetric reflection from the surface of a perfect crystal. The diffraction vector, **g**, is represented by OG. Its magnitude (taken as the reciprocal of the interplanar spacing of the Bragg-reflecting planes) and its direction are ideally well defined. Consequently, the Brillouin zone boundary BB', perpendicularly bisecting OG, is ideally well defined in position and orientation. A highly collimated inci-

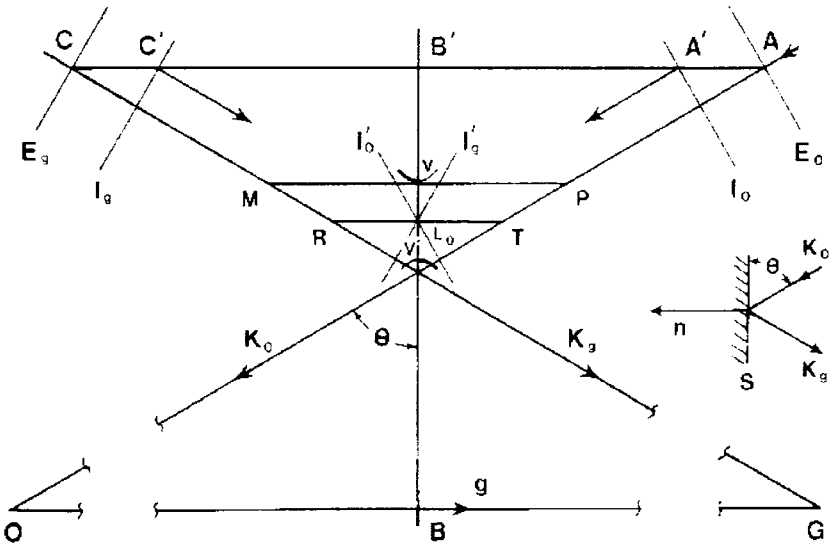

Fig. 1. Reciprocal-space geometry applying in symmetric Bragg reflection from a crystal surface, as detailed in the text. The inset on the right shows real-space geometry of wavevectors incident ($\mathbf{K}_0$) and reflected ($\mathbf{K}_g$) at the crystal surface S whose inward-drawn normal is **n**. The segments of the dispersion-surface hyperbolae drawn have asymptotes I'_0 and I'_g intersecting at the Lorentz point L_0 on BB'. The dispersion-surface frequency is that of the vacuum (*i.e.* external) wavevectors having lengths OT and RG. R and T lying on the line parallel to **n** that passes through L_0, and $TL_0 = L_0R = AA' = CC' = K\delta\operatorname{cosec}\theta$ where $1 - \delta$ is the X-ray refractive index. (The crystal is assumed to be thick, so that only the heavily drawn halves of the dispersion-surface hyperbolae can be excited.)

dent wavevector $\mathbf{K}_0$, magnitude λ^{-1}, is fixed in direction relative to OG and BB', making angle θ with BB'. Consider first such a value of $|\mathbf{K}_0|$, represented by the length AO, that places A some distance from BB' and hence relatively far from strong excitation of a Bragg reflection. The trace of the tangent plane to the K_0 wave surface at A is indicated by E_0. I_0 indicates that corresponding to the wave surface of k_0, the incident wave refracted into the crystal; the ratio $|\mathbf{k}_0|/|\mathbf{K}_0|$ is given by the normal, real X-ray refractive index, $1 - \delta$, where δ is real and typically 10^{-6} to 10^{-5}. The basic Snell's law construction, extending $AA'B'C'C$ parallel to $\mathbf{n}$, defines the direction of $\mathbf{k}_0$, $A'O$, and of the notional Bragg-reflected rays within the crystal, $\mathbf{k}_g$, $C'G$, and outside it, $\mathbf{K}_g$, CG. (E_g is the trace of the tangent plane to the K_g wave surface at C and I_g correspondingly to the k_g wave surface at C'.) Note that, as A moves up or down the $\mathbf{K}_0$ axis according to the value of λ^{-1}, C moves proportionately up or down the $\mathbf{K}_g$ axis, maintaining the same inclination θ to BB'. Additionally, as long as there is negligible excitation of the Bragg reflection, the direction of $\mathbf{k}_0$ remains given by $\mathbf{K}_0 - (\mathbf{AA}')$ and of $\mathbf{k}_g$ by $\mathbf{K}_g - (\mathbf{CC}')$, with $AA' = CC' = K\delta\mathrm{cosec}\,\theta$.

Consider next the case when Bragg reflection is strongly excited. One is then concerned with magnitudes $|\mathbf{K}_0|$ close to TO. As Fig. 1 shows, TO is that incident wavevector that lies at the centre of the range of total reflection and RG is the reflected wavevector similarly characterized: $TL_0 = AA'$ and $RL_0 = CC'$. The tangent planes to the k_0 and k_g spheres at L_0 on BB' are asymptotes of the dispersion-surface hyperbolae. The vertices of the upper and lower branches are labelled V and V', respectively; they lie on BB'. Although the dispersion surface drawn applies strictly only to the frequency of OT, the range of K_0 values needed to span the range of strong Bragg reflection is so small relatively that invariance of dispersion-surface geometry can be assumed. Thus an incident wavevector of larger magnitude, PO, that lies at one end of the range of total reflection is that for which the line drawn through P parallel to $\mathbf{n}$ is tangent at V, and intersects the $\mathbf{K}_g$ axis at M. The corresponding crystal wavevectors have directions **VO** and **VG**, which are not the same as **A'O** and **C'G**. However, the emerging Bragg-reflected wave has direction **MG** collinear with **CG**. The diametrical distance VV' will determine the range of wavelengths in the band of totally reflected X-rays, but the orientation of all these reflected rays remains invariant as that of CG, which is no less sharply defined than the orientation of the incident ray AO, provided the lateral dimensions of the specimen are not so small as to significantly diffraction-broaden the angular range of $\mathbf{K}_g$ rays.

3. Symmetric Laue case

To illustrate symmetric Laue-case transmission, a simpler drawing, Fig. 2, serves. It suffices to include possible vacuum wave surfaces only, omitting the dispersion-surface hyperbolae and their asymptotic surfaces, the latter all being similarly translated downwards parallel to $B'B$ by $K\delta\sec\theta$ relative to their respective vacuum wave surfaces. Fig. 2 shows three possible Laue points, L, L' and L''. Point L is on the intersection of AO and BB'. Hence the incident wavevector of length LO satisfies the Bragg condition exactly. When $\mathbf{K}_0$ has length $P'O$ the exact Bragg condition wavevector for this wavelength is $L'O$. Since $P'O$ makes a smaller angle with BB' than $L'O$ does, its glancing angle is less than the Bragg angle (a case of deviation parameter $w < 0$). On the other hand, when $\mathbf{K}_0$ has length $Q''O$, the Bragg condition wavevector would be $L''O$. The inclination of $Q''O$ to BB' exceeds that of $L''O$ (and $w > 0$ correspondingly). The parameter w is a convenient measure of departure from peak Bragg reflection. Assuming zero absorption, the transmitted Bragg-reflected intensity, $P_g(w)$, is related to the peak value $P_g(0)$ at $w = 0$ by $P_g(w)/P_g(0) = (1 + w^2)^{-1}$. Hence the range $-1 \leq w \leq 1$ corresponds to the angular full width at half-maximum (FWHM) of $P_g(w)$ in this assumed zero-absorption case. If the orientation of incident wavevector $\mathbf{K}_0$ *were* allowed to vary, then the FWHM range of $P_g(w)$ would be spanned when the orientation of $\mathbf{K}_0$ changed from PO, chosen to correspond to $w = -1$, to QO, where $w = 1$. The standard construction, producing lines through P and Q parallel to $\mathbf{n}$ so as to intersect the K_g wave surface, would then determine the corresponding $\mathbf{K}_g$ vectors as **MG** and **NG**. The angular ranges PQ/LO and MN/LG are obviously equal. (To give a scale to the segments of wave surfaces drawn, recall that when $w = \pm 1$, the geometry of the dispersion-surface hyperbolae makes the distances PM and NQ equal to the inter-vertex diameter VV', labelled in Fig. 1, and this diameter VV' is the reciprocal of the extinction distance, ξ_g.) Prolonging PM downwards to make intersections P' and M' shows that for $|\mathbf{K}_0| = P'O$ the parameter $w = 1$, and the corresponding $\mathbf{K}_g$ direction is $M'G$. Further, upward prolongation of QN to make intersections Q'' and N'' shows that $w = 1$ for $|\mathbf{K}_0| = Q''O$, and then the

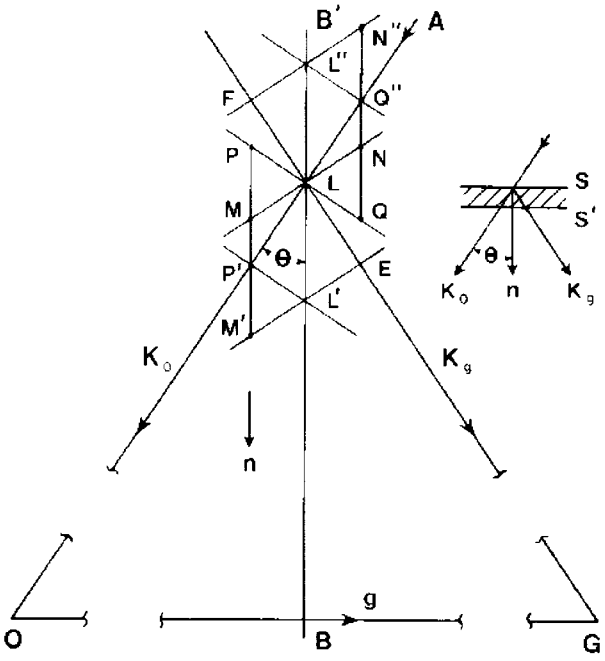

Fig. 2. Reciprocal-space geometry in symmetric Laue-case transmission. As in Fig. 1, the diffraction vector $\mathbf{g}$ is represented by OG and the strictly collimated incident wavevectors $\mathbf{K}_0$ are parallel to AO. BB' is the Brillouin zone boundary. The inset on the right shows real-space geometry of $\mathbf{K}_0$, $\mathbf{K}_g$ and the parallel-sided plate specimen having X-ray entrance and X-ray exit surfaces S and S', respectively. The common normal to both S and S', drawn inward from S, is $\mathbf{n}$. Only the vacuum wave-surface traces belonging to possible incident and diffracted waves are drawn, for simplicity.

corresponding $\mathbf{K}_g$ direction is $N''G$. Thus, as the magnitude of $|\mathbf{K}_0|$ varies so as to span the FWHM range of Bragg-reflection intensity, the diffracted wavevector $\mathbf{K}_g$ rotates through the angle

$$(M'E + FN'')/LG = 2MN/LG = 2\xi_g^{-1}\operatorname{cosec}\theta.$$

This represents very different behaviour of $\mathbf{K}_g$ compared with that exhibited in the case of a symmetric surface reflection, described earlier.

4. Asymmetric Bragg case

Return now to Bragg-case reflection from a perfect crystal. As before, consider reflection of an ideally strictly collimated polychromatic incident beam. The question that needs to be answered is to what extent the valuable property of invariance of direction of Bragg-reflected rays, demonstrated above in the case of symmetric reflection, is retained when reflection becomes asymmetric. Fig. 3 shows again the dispersion-surface geometry for Bragg reflection of rays incident at angle θ, but here the crystal surface is rotated by angle α anticlockwise relative to the Bragg planes. The range of $|\mathbf{K}_0|$ values totally reflected (again assuming zero absorption) lies between DO and $D'O$, where lines DF and $D'F'$ drawn parallel to $\mathbf{n}$ are tangent to the upper and lower branches of the dispersion surface, respectively. Point F lies on the K_g wave surface whose radius $EG = DO$, and F' on that whose radius $E'G = D'O$. Both the Bragg-reflected wave FG produced by the incident wave DO and the Bragg-reflected wave $F'G$ produced by the incident wave $D'O$ are deviated from direction CG; the angle between them, $(FE - F'E')/K$, is to be calculated. It is proportional to the perpendicular distance between tangents DF and $D'F'$, which is given by the length of their mutual perpendicular HH' passing through L_0. Note that $DD' = HH'\sec(\theta + \alpha)$. From similar triangles in Fig. 3, $EF/DX = E'F'/D'X$, so that $EF - E'F' = DD'(EF/DX)$. In the triangle DEF, $EF/\sin\alpha = ED/\sin(\theta - \alpha)$ and $ED = 2DX\sin\theta$. Thus

$$\begin{aligned} EF &= ED\sin\alpha\operatorname{cosec}(\theta - \alpha) \\ &= 2DX\sin\alpha\sin\theta\operatorname{cosec}(\theta - \alpha). \end{aligned} \quad (1)$$

Inserting the ratio EF/DX from (1) into the expression for $EF - E'F'$ gives

$$\begin{aligned} EF - E'F' &= 2DD'\sin\alpha\sin\theta\operatorname{cosec}(\theta - \alpha) \\ &= 2HH'\sin\alpha\sin\theta\operatorname{cosec}(\theta - \alpha)\sec(\theta + \alpha) \\ &= 2HH'\sin\alpha\sin\theta/(\sin\theta\cos\theta - \sin\alpha\cos\alpha). \end{aligned} \quad (2)$$

For the case when α is small and θ is not close to $\pi/2$, (2) reduces to the approximation

$$EF - E'F' \simeq 2\alpha HH'\sec\theta. \quad (3)$$

The relation between HH', the distance between the dispersion-surface tangents DF and $D'F'$, and the distance between tangents at the vertices, *i.e.* the inter-vertex diameter VV', can be found from the geometrical properties of hyperbolae or extracted from standard X-ray dynamical/theoretical treatments of asymmetric Bragg-case reflection (James, 1963). Here, concentrating on small values of $|\alpha|$, a reasonable estimate of the magnitude of $EF - E'F'$ can be derived simply by replacing HH' by VV', the basic parameter ξ_g^{-1}, which is seen from Fig. 3 to differ little from HH' for low values of $|\alpha|$. Then, denoting the angle $(EF - E'F')/K$ $\Delta\theta_g$, the simple approximation obtained for its magnitude is

$$\Delta\theta_g = 2|\alpha|\xi_g^{-1}\lambda\sec\theta. \quad (4)$$

To appreciate the scale of $\Delta\theta_g$, it may be compared with the angular range, $\Delta\theta_0$, of total reflection of incident monochromatic X-rays in the symmetric Bragg case, zero absorption, which is given by $\Delta\theta_0 = \xi_g^{-1}\lambda\operatorname{cosec}\theta$. The ratio of the two angles is

$$\Delta\theta_g/\Delta\theta_0 = 4|\alpha|\operatorname{cosec}2\theta, \quad (5)$$

which is lowest at $2\theta = 90°$. The undesirability of using high Bragg angles is emphasized by substituting in (4) the component factors in ξ_g^{-1}. For σ-mode polarization, $\xi_g^{-1} = r_e F_g\lambda/\pi V\cos\theta$, where $r_e = e^2/mc^2$, F_g is the structure factor of

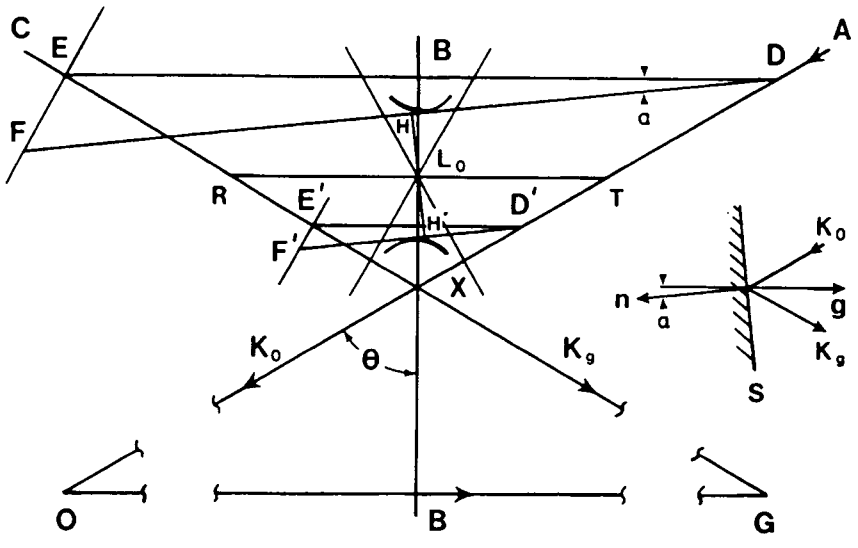

Fig. 3. Reciprocal-space constructions for asymmetric Bragg reflection from a crystal surface, explained in the text. The inset on the right shows real-space geometry of $\mathbf{K}_0$, $\mathbf{K}_g$ and the crystal surface S whose inward-drawn normal is $\mathbf{n}$. Surface S is inclined at angle α to the Bragg-reflecting planes. The sense of α is taken positive when similar to the deviation of $\mathbf{K}_0$ into $\mathbf{K}_g$ by the angle 2θ. The asymmetry factor, b, has magnitude $|\mathbf{K}_0\cdot\mathbf{n}/\mathbf{K}_g\cdot\mathbf{n}| = \sin(\alpha + \theta)/\sin(\alpha - \theta)$. As in Figs. 1 and 2, BB' is the perpendicular bisector of the reciprocal-lattice vector OG. Highly collimated polychromatic incident wavevectors $\mathbf{K}_0$ have direction AO making angle θ with BB', and the reflection of AO in BB' provides the nominal direction CG of reflected wavevectors $\mathbf{K}_g$. CG and AO intersect at X on BB'. R, L_0 and T are the same as in Fig. 1.

the reflection concerned and V is the unit-cell volume. Then (4) becomes

$$\Delta\theta_g = 2|\alpha|r_e(F_g\lambda^2/\pi V)\sec^2\theta. \quad (6)$$

5. Conclusion

The need for quantitative knowledge of the 'perfect-crystal' value of $\Delta\theta_g$ given by (6), even if only approximate, comes to the fore in experiments assessing crystal quality from the angular spread observed in the diffracted rays that contribute to the X-ray topographic image of the crystal when collimated polychromatic radiation is incident. In particular, the new technique of X-ray reticulography (Lang & Makepeace, 1996), which is capable of measuring microradian-magnitude variations in diffracted-ray orientation point by point over the topographic image and hence of measuring crystal-lattice misorientations point by point with similar sensitivity, will realize its maximum potential when used in the symmetric Bragg-case reflection mode. If it is not experimentally possible to use symmetric Bragg-case reflection, then Bragg angles approaching $\pi/2$ should be avoided in order to keep $\Delta\theta_g$ low with a given α.

There are alternative routes to the findings given above for the Bragg case. Reflection of polychromatic synchrotron radiation by a flat perfect crystal is briefly dealt with in a more general but rather abstract way among the analyses of various synchrotron X-ray optical systems discussed by Matsushita & Kaminaga (1980*a*,*b*); and Brauer, Stephenson & Sutton (1995) illustrate the application of the DuMond diagram to the case of collimated polychromatic incident radiation. The approach adopted here, which explicitly applies the principle of continuity of tangential components of wavevectors at crystal boundaries in both reflection and transmission cases, is presented as an appropriate and transparent way of dealing with the synchrotron X-ray topographic diffraction geometrical questions addressed.

References

Brauer, S., Stephenson, G. B. & Sutton, M. (1995). *J. Synchrotron Rad.* **2**, 163–173.
James, R. W. (1963). *Solid State Phys.* **15**, 53–219.
Lang, A. R. & Makepeace, A. P. W. (1996). *J. Synchrotron Rad.* **3**, 313–315.
Matsushita, T. & Kaminaga, U. (1980*a*). *J. Appl. Cryst.* **13**, 465–471.
Matsushita, T. & Kaminaga, U. (1980*b*). *J. Appl. Cryst.* **13**, 472–478.